Reprinted without change of pagination from *Symposium on Measurement in Unsteady Flow*,
Presented at the ASME Hydraulic Division Conference, May 21-23, 1962.

Technical Report No. 32-229

Application of Hot-Wire Techniques in Unsteady Compressible Flows

Thomas Vrebalovich

This paper presents results of one phase of research carried out by the Jet Propulsion Laboratory, California Institute of Technology, under Contract No. NAS 7-100, sponsored by the National Aeronautics and Space Administration.

JET PROPULSION LABORATORY
CALIFORNIA INSTITUTE OF TECHNOLOGY
PASADENA, CALIFORNIA

May, 1962

Author's Reprint – Presented at the ASME Hydraulic Division Conference, May 21-23, 1962 and published in *Symposium on Measurement in Unsteady Flow* by The American Society of Mechanical Engineers, 345 East 47th Street, New York 17, New York.

APPLICATION OF HOT-WIRE TECHNIQUES IN UNSTEADY COMPRESSIBLE FLOWS*

Thomas Vrebalovich

Abstract

The interpretation of hot-wire voltage fluctuations induced by an unsteady compressible flow field is presented. The use of fluctuation mode diagrams to determine the type and amplitude of disturbances detected in an unsteady flow is illustrated. Some of the examples are the following: unsteady flow in an oscillating compressible laminar boundary layer, the potential field near such a boundary layer, and the disturbances present in a supersonic wind tunnel. The results are compared both with theory and with other measuring techniques. A practical computational scheme is given for the determination of unsteady flow quantities from hot-wire results.

Introduction

The extension of the hot-wire technique from low-speed to high-speed compressible flows provides a useful tool for determining fluctuations in compressible flow fields. The work of Kovásznay [1, 2, 3] and Morkovin [4] gives practical computational schemes for determining the unsteady quantities in supersonic flow fields. This, plus the experimental determination of hot-wire heat loss and recovery temperature relations [1, 2, 5, 6], enables fluctuation measurements to be made. The high frequencies present in supersonic flow fields require increased frequency response in the new hot-wire amplifiers, and this is now attainable [3, 7, 8]. The increased frequency range also demands the use of extremely fine wires to reduce the thermal lag and to give reasonable signal-to-noise ratios.

With the development of the method of interpreting fluctuation measurements, with the law for the loss of heat experimentally determined, with the improvement in hot-wire amplifier frequency response, and with the feasibility of using extremely fine wires, it is now possible to determine the unsteady flow quantities present in many supersonic flow fields.

In order to show the *practicability* and the *applicability* of the hot-wire technique at supersonic speeds, several experiments which were conducted at the Jet Propulsion Laboratory will be described. In some of these experiments different techniques, all involving the use of a hot wire, were applied to get the same result. The measurements also gave insight into the sources of the unsteady flow fields present. Some comparisons of results were made with the theoretical solutions.

This paper presents the results of one phase of research carried out at the Jet Propulsion Laboratory, California Institute of Technology, under Contract NAS 7-100, sponsored by the National Aeronautics and Space Administration.

Fluctuation Sensitivities and Mode Diagrams

In order to make fluctuation measurements with a hot wire, it is necessary to know a steady-state heat loss law. Using simple dimensional analysis, it may be shown that $Nu = Nu(M, Re, \tau_{wr})$, where Nu is the Nusselt number, M the free-stream Mach number, Re the wire Reynolds number, and τ_{wr} a wire overheat parameter. Laufer and McClellan [5] found that for $M > 1.3$, $Nu_2 = Nu_2(Re_2, \tau_{wr})$ only where air viscosity and conductivity were determined from the static temperature T_2 behind the normal shock wave. Since T_2 can be fairly well approximated by the total temperature T_T, it is more convenient to use the total temperature instead of T_2 as the reference temperature in the heat loss law. The Nusselt number is still a function of Re_T only and reasonably independent of Mach number for $M > 1.2$ [4 and 7].

The Nusselt number approaches a constant value as the wire overheat value goes to zero, and the unheated wire equilibrium temperature is the recovery temperature T_r. Experimentally, it is found that $\eta = \eta(M, Re_T) = T_r/T_T$. The effect of neglecting the Mach number dependence results in a small error in the fluctuation sensitivities for $M > 1.5$.

Assuming that the time constant due to the heat capacity of the hot wire has been determined experimentally (square wave method, [8]), the basic hot-wire equation may be written as

$$\Delta e = -\Delta e_\rho \frac{\Delta\rho}{\rho} - \Delta e_u \frac{\Delta u}{U} + \Delta e_T \frac{\Delta T_T}{T_T}$$

where Δe is the voltage fluctuation across the hot wire; $\Delta\rho$, Δu, and ΔT_T are the fluctuating components of the mean flow, density ρ, velocity U, and total temperature T_T; and Δe_ρ, Δe_u, and Δe_T are the sensitivity coefficients of the hot wire. From Morkovin [4], the sensitivity coefficients are given as

$$\Delta e_\rho = eE' \left[A'_w \frac{Re_T}{Nu_T} \frac{\partial Nu_T}{\partial Re_T} - \frac{A'_w}{\tau_{wr}} \frac{Re_T}{\eta} \frac{\partial \eta}{\partial Re_T} \right]$$

$$\Delta e_u = \Delta e_\rho + eE' \left[\frac{A'_w}{\alpha} \left(\frac{M}{Nu_T} \frac{\partial Nu_T}{\partial M} - \frac{1}{\tau_{wr}} \frac{M}{\eta} \frac{\partial \eta}{\partial M} \right) \right]$$

$$\Delta e_T = e E' \left[K + A'_w \left(K - 1 - n_T + m_T \frac{Re_T}{Nu_T} \frac{\partial Nu_T}{\partial Re_T} + \frac{1}{2\alpha} \frac{M}{Nu_T} \frac{\partial Nu_T}{\partial M} \right) \right.$$

$$\left. - \frac{A'_w}{\tau_{wr}} \left(\frac{1}{2\alpha} \frac{M}{\eta} \frac{\partial \eta}{\partial M} + m_T \frac{Re_T}{\eta} \frac{\partial \eta}{\partial Re_T} \right) \right]$$

where e is the mean voltage across the wire. The various parameters can be calibrated directly; their definition and method of calibration will be found in the Appendix. For most applications the Nusselt vs Reynolds number and recovery temperature vs Reynolds number relations need not be determined *in situ*. Provided that end loss effects due to finite wire length are taken into account, the Nusselt vs Reynolds relation for the heat loss as determined by Laufer and McClellan [5] and others may be used for calculating the quantity $(Re/Nu)(\partial Nu/\partial Re)$. For a wire Reynolds number greater than 1 the recovery temperature data of Laufer and McClellan are adequate.

For $M > 1.2$, $\Delta e_u = \Delta e_\rho = \Delta e_m$ where Δe_m is the sensitivity to mass flow fluctuations. The hot-wire equation may then be written as

$$\Delta e = -\Delta e_m \frac{\Delta m}{m} + e_T \frac{\Delta T_T}{T_T}$$

where

$$\frac{\Delta m}{m} = \frac{\Delta(\rho_u)}{\rho_U} = \frac{\Delta \rho}{\rho} + \frac{\Delta u}{U}$$

The mean square of this hot-wire equation is

$$\left(\frac{\Delta e'}{\Delta e_T} \right)^2 = \left(\frac{\Delta T'_T}{T_T} \right)^2 - 2 \left(\frac{\Delta e_m}{\Delta e_T} \right) \frac{\overline{\Delta m \Delta T_T}}{m T_T} + \left(\frac{\Delta e_m}{\Delta e_T} \right)^2 \left(\frac{\Delta m'}{m} \right)^2$$

or

$$\left(\frac{\Delta e'}{\Delta e_T} \right)^2 = \left(\frac{\Delta T'_T}{T_T} \right)^2 - 2 \frac{\Delta e_m}{\Delta e_T} R_{m_T} \frac{\Delta m'}{m} \frac{\Delta T'_T}{T_T} + \left(\frac{\Delta e_m}{\Delta e_T} \right)^2 \left(\frac{\Delta m'}{m} \right)^2$$

where

$$R_{m_T} = \frac{\overline{\Delta m \Delta T_T}}{\Delta m' \Delta T'_T}$$

is the correlation coefficient, and the prime denotes the root mean square of the fluctuation; e.g.,

$$\Delta e' = \sqrt{\overline{(\Delta e)^2}}.$$

The three unknowns in this equation are $\Delta T'_T$, $\Delta m'$, and R_{m_T}. If the fluctuation measurements are carried out at three overheat values, three sets of sensitivity coefficients are obtained. The resulting three independent equations may be solved for the three unknowns.

In practice the hot wire may be operated at more than three overheat values and the results plotted in the fluctuation mode diagram employed by Kovásznay [2]. The fluctuation mode diagram is a plot of $\Delta e'/\Delta e_T$ vs $\Delta e_m/\Delta e_T$. As can be seen from the mean square of the hot-wire equation given above, a plot of $\Delta e'/\Delta e_T$ vs $\Delta e_m/\Delta e_T$ must be a conic section with the three unknowns involved as the constant coefficients of the quadratic equation. Therefore, only three unknown quantities may be determined by this method, and operating at many overheat values only helps reduce the scatter. No further information may be obtained even from the original form of the equation, which in the mean square would have six unknowns ($\Delta\rho'$, $\Delta u'$, $\Delta T'$, $\overline{\Delta\rho \Delta u}$, $\overline{\Delta\rho \Delta T}$, and $\overline{\Delta u \Delta T}$).

Unfortunately, the mass flow and total temperature fluctuations are not the characteristic parameters of an unsteady supersonic flow field. The application of small-perturbation analysis to the equations for conservation of momentum, energy, and mass, the equation of state, and the division of the fluctuating flow field into its irrotational, solenoidal, and harmonic parts leads to a separation of the fluctuating flow quantities into three modes [2, 4]. These are the vorticity r, entropy σ, and sound π modes. If the fluctuation field is strong, there are moderate second-order interactions; whereas, if the field is weak, the modes satisfy separate linear differential equations. The hot-wire equation then becomes

$$\Delta e = \sigma \cdot \Delta e_\sigma + r \cdot \Delta e_r + \pi \cdot \Delta e_\pi$$

The new sensitivity coefficients are given as

$$\Delta e_\sigma = \Delta e_\rho + \alpha \Delta e_T$$

$$\Delta e_r = \beta \Delta e_T - \Delta e_u$$

$$\Delta e_\pi = \alpha(\gamma - 1)(1 - n_x M) \Delta e_T - \frac{n_x}{M} \Delta e_u - \Delta e_\rho$$

where α and β are functions of Mach number M (see Appendix) and the ratio of specific heats γ. In the sound mode fluctuation sensitivity, n_x is the direction cosine of the normal to a plane sound wave. It is possible for n_x to have more than one value if there are several sound wave directions.

The fluctuation variables given as a function of the modes are

$$\frac{\Delta T}{T} = \sigma + (\gamma - 1)\pi$$

$$\frac{\Delta \rho}{\rho} = -\sigma + \pi$$

$$\frac{\Delta u}{U} = \tau + \frac{n_x \pi}{M}$$

$$\frac{\Delta P}{P} = \gamma \pi$$

$$\frac{\Delta T_T}{T} = \alpha\sigma + \beta\tau + \left[(\gamma - 1)\alpha + \frac{\beta n_x}{M}\right]\pi$$

$$\frac{\Delta m}{m} = -\sigma + \tau + \left(1 - \frac{n_x}{M}\right)\pi$$

In general it is not possible to decompose hot-wire measurements into the individual modes. Morkovin [4] suggested a scheme for determining the entropy, vorticity, and sound modes; this method is not only useful when at least one of the modes or certain of the correlations may be neglected, but gives insight into the fluctuations which may be present. By plotting the fluctuation mode diagram of $\Delta e'/\Delta e_\sigma$ vs $\Delta e_\tau/\Delta e_\sigma$ it is sometimes possible to determine which fluctuations or correlations may be neglected. The usual shape of the diagram in this coordinate system is the rectangular hyperbola, and the detailed method for graphically reducing the data is described by Morkovin [4].

Experimental Equipment

The experiments were conducted in the Jet Propulsion Laboratory 18 × 20-in. supersonic wind tunnel. A detailed description of the equipment used may be found in [8, 9, and 10].

All of the hot wires were 90% platinum and 10% rhodium with diameters of 0.00005 or 0.0001 in. and were 0.010 to 0.020 in. long. A typical boundary-layer probe consisted of a razor blade 0.060 in. wide and 0.004 in. thick attached to a strut. Two jeweler's broaches were glued to the blade and extended 0.050 in. in front of it as shown in Fig. 1.

The Shapiro and Edwards Model 50B constant-current hot-wire set had an amplifier with a frequency response up to 300 kc. It had an equivalent input noise less than that of a 1000-ohm resistance and an input transformer which could reduce the input noise effect by a factor of at least four.

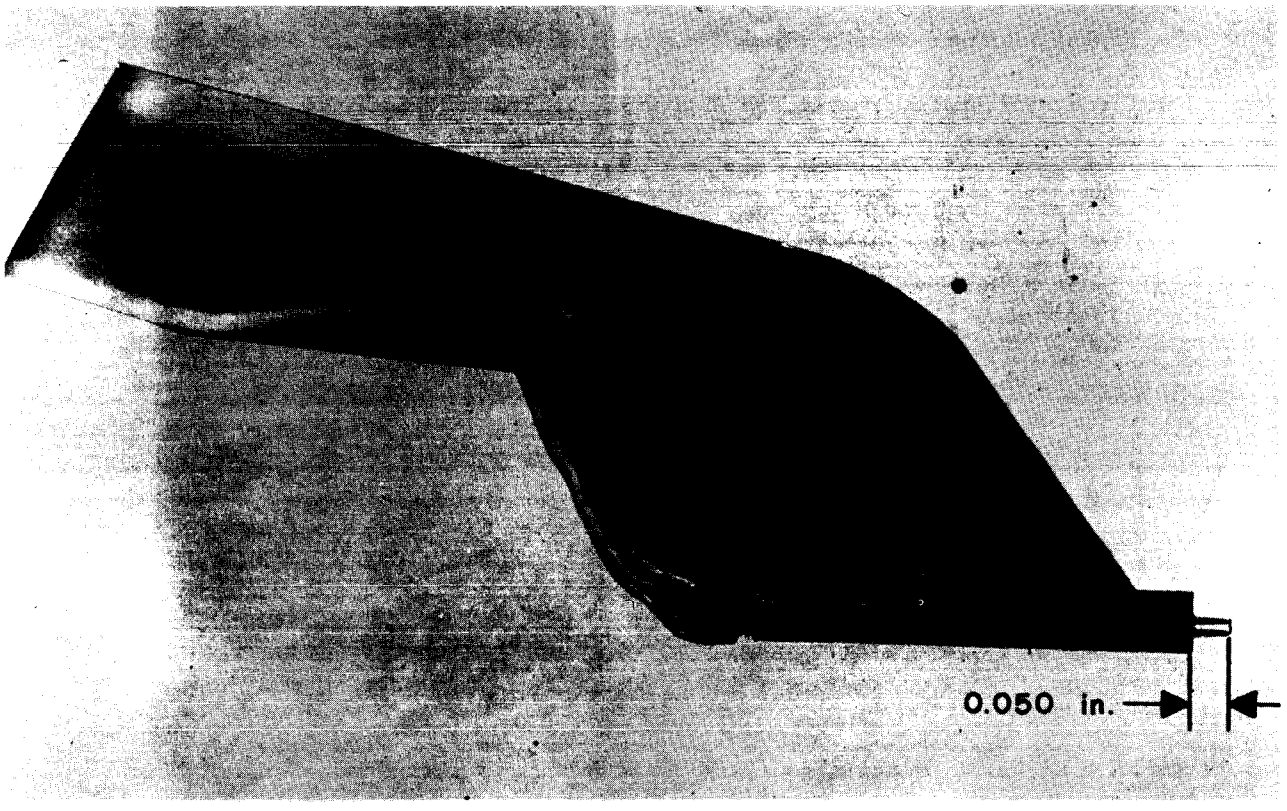

Figure 1. Hot-wire probe

Experimental Results

1. *The Propagation Velocity of a Disturbance in a Supersonic Laminar Boundary Layer on a Flat Plate.* One of the problems encountered in the laminar boundary layer stability program [9] was that of determining the propagation velocity of a disturbance in the layer. Disturbances originating near the leading edge of the plate propagate along the plate as Tollmien waves at their own propagation velocity. A disturbance generator near the leading edge of a flat plate was a source of single-frequency disturbances up to 90 kc. A photocell in the flat plate near the disturbance generator monitored the frequency of the artificial disturbance. A hot wire in or near the boundary layer also could detect the artificial disturbance.

By taking the mean square of the difference of the photocell and hot-wire output at the artificial disturbance frequency and plotting this difference as the hot wire was moved aft on the flat plate, a curve like that shown in Fig. 2 could be obtained. The maxima correspond to out-of-phase signals and the minima to in-phase signals. The distance between maxima (or minima) is the wavelength of the signal. The propagation velocity (wave velocity) is then

$$U_c = \lambda f = 0.60\ U$$

where λ is the wavelength, f the frequency of the disturbance, and U the free-stream velocity.

Of incidental value to the above discussion, but important in illustrating the versatility of the hot wire, is the second curve on Fig. 2. This curve was obtained by feeding the galvanometer output of the hot-wire bridge to a servo system which kept the resistance of the wire constant and the resistance bridge balanced by moving the wire vertically in the boundary layer. Since the laminar boundary layer profiles were similar, the wire was maintained at a constant percentage of the boundary layer thickness as the wire was moved aft. A laminar boundary layer grows parabolically on a flat plate, which is confirmed by the second curve in Fig. 2.

There is a second technique for determining the propagation velocity which is not as accurate but requires only a single hot-wire output and the fluctuation mode diagram. The boundary layer oscillation may be considered to be a moving wavy wall. For a stationary wavy wall with flow moving past, the pressure coefficient [10] is

$$C_p = -\frac{2\Delta u}{U_r}$$

and

$$C_p = \frac{\Delta P}{\frac{\gamma}{2} M_r^2\ P}$$

and therefore

$$-\frac{\Delta u}{U_r} = \frac{\Delta P}{\frac{\gamma}{2} M_r^2\ P}$$

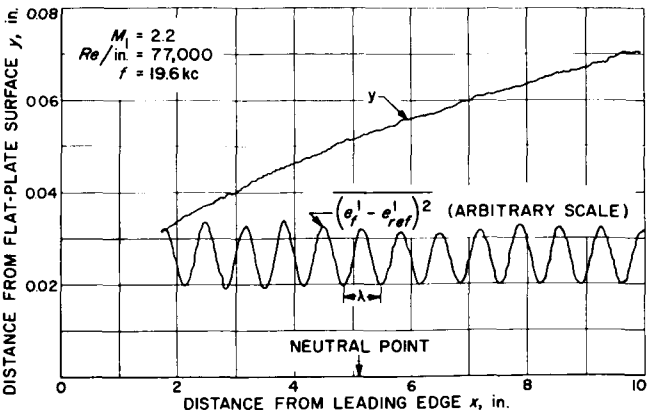

Figure 2. Wavelength measurement of an artificial disturbance

or

$$\frac{\Delta u'}{U_r} = \frac{\Delta P'}{\frac{\gamma}{2} M_r^2\ P}$$

in terms of the rms fluctuation, where U_r is the relative velocity past the stationary wavy wall, $M_r = U_r/a$, a is the local speed of sound, and P the mean static pressure. For a wavy wall moving at a propagation velocity U_c, the free-stream velocity is then

$$U = U_r + U_c$$

Substituting this in the above equation,

$$\frac{U_c}{U} = 1 - \frac{\frac{\Delta P'}{P}}{\gamma M^2 \frac{\Delta u'}{U}}$$

where M is the free-stream Mach number. Thus by measuring $\Delta P'/P$ and $\Delta u'/U$, U_c may be calculated. Furthermore, outside the boundary layer an isentropic relation between fluctuations may be assumed:

$$\frac{\Delta P}{P} = \frac{\gamma \Delta \rho}{\rho} = \frac{\gamma}{\gamma - 1} \frac{\Delta T}{T}$$

Examination of the mode diagram of the artificial disturbance in Fig. 3 taken outside the boundary layer indicates that the plot of $\Delta e'/\Delta e_T$ vs $\Delta e_m/\Delta e_T$ is a straight line. The significance of this becomes apparent from the mean square of the hot-wire equation

$$\left(\frac{\Delta e'}{\Delta e_T}\right)^2 =$$

$$\left(\frac{\Delta T_T'}{T_T}\right)^2 - 2\frac{\Delta e_m}{\Delta e_T} R_{m_T} \frac{\Delta T_T'\ \Delta m'}{T_T m} + \left(\frac{\Delta e_m}{\Delta e_T} \frac{\Delta m'}{m}\right)^2$$

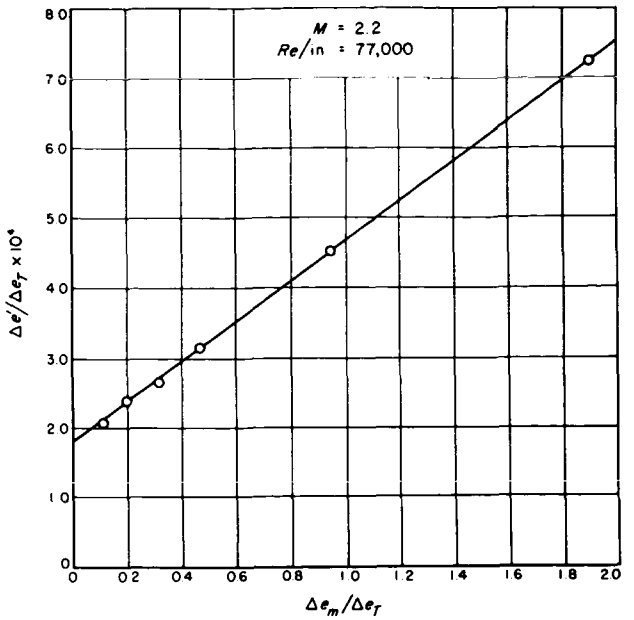

Figure 3. Fluctuation mode diagram, $\Delta e'/\Delta e_T$ vs $\Delta e_m/\Delta e_T$

where the correlation coefficient is

$$R_{m_T} = \frac{\overline{\Delta T_T \, \Delta m}}{\Delta T_T' \, \Delta m'}$$

Since the mode diagram is a straight line, $R_{m_T} = -1$, which indicates that Δm and ΔT_T are anticorrelated, and that obviously

$$\frac{\Delta e'}{\Delta e_T} = \frac{\Delta T_T'}{T_T} + \frac{\Delta e_m}{\Delta e_T}\frac{\Delta m'}{m}$$

It is clear then that the intercept of the straight line is $\Delta T_T'/T_T$ and the slope is $\Delta m'/m$.

From the isentropic relations and

$$\frac{\Delta m}{m} = \frac{\Delta u}{U} + \frac{\Delta \rho}{\rho}$$

$$\frac{\Delta T_T}{T_T} = \alpha \frac{\Delta T}{T} + \beta \frac{\Delta u}{U}$$

the following is obtained:

$$\frac{\Delta m}{m} = \frac{\Delta u}{U} + \frac{1}{\gamma}\frac{\Delta P}{P}$$

$$\frac{\Delta T_T}{T_T} = \alpha(\gamma - 1)\left(\frac{\Delta P}{P} + M^2 \frac{\Delta u}{U}\right)$$

Solving these two equations for $\Delta u/U$ and $\Delta P/P$ and taking rms values of the fluctuations, $\Delta u'/U$ and $\Delta P'/P$ are found as a function of the known quantities $\Delta m'/m$ and $\Delta T_T'/T_T$.

The propagation velocity determined from the use of the mode diagram is $U_c/U = 0.60$, and this result compares well with $U_c/U = 0.62$, which is both the theoretical value and that obtained by the first method described. In the latter method the use of the mode diagram plus the isentropic relations allowed a complete determination of all of the fluctuating quantities outside the edge of the oscillating laminar boundary layer. From the C_p for a wavy wall, it was then possible to calculate the velocity of propagation of a Tollmien wave of a given frequency.

2. *Amplitude Distribution of Disturbances Across a Supersonic Laminar Boundary Layer on a Flat Plate.* The fluctuation profile of the oscillation present in an artificially disturbed laminar boundary layer was determined in [8]. In Example 1, all of the fluctuating quantities were determined outside the layer. Clearly the isentropic relations will not be valid inside the layer and another relation must be determined. By a qualitative argument, which was substantiated by the theory, it seemed likely that the pressure fluctuations would be constant throughout the layer.

The mass flow and total temperature fluctuation profiles were determined from mode diagrams and are plotted in Fig. 4. The solution is shown only for the supersonic region. The mode diagram and the assumption of constant pressure fluctuations through the layer result in two roots and an undetermined phase relation between the pressure and velocity (or temperature) fluctuations. Near the outer edge of the layer the phase could be determined by matching it to the one just outside the layer. The two roots define two completely different sets of velocity and temperature distributions. The points shown in Fig. 5 correspond to the roots of the hot-wire equation which were nearest the theoretical curves. With respect to the pressure fluctuations which are plotted in a positive sense, all the points plotted in a positive sense are in phase and those in a negative sense are 180 deg out of phase with the pressure fluctuations. The results of the chosen set of roots compare favorably with the theoretical solution.

3. *Free-Stream Fluctuations in a Supersonic Wind*

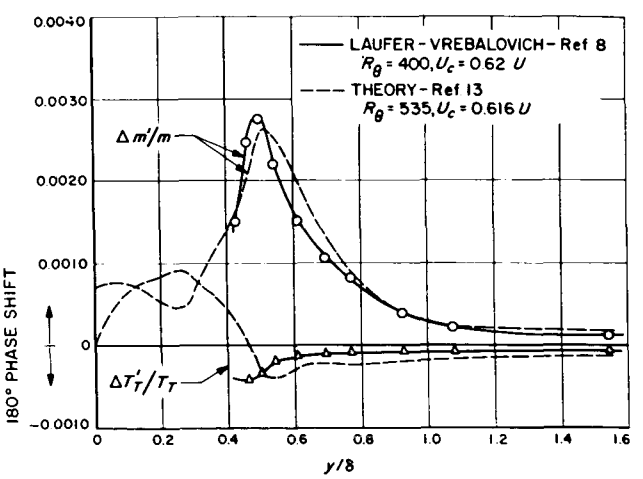

Figure 4. Mass flow and total temperature fluctuations in a laminar boundary layer

Tunnel. In low-speed wind tunnels the turbulence level of the free stream has strongly affected certain types of experiments, and it is expected that fluctuations in a supersonic flow field will also be important. The results of experiments conducted in the JPL supersonic wind tunnels indicated that the fluctuations in the free stream are sound radiation from the turbulent boundary layers on the walls of the tunnel [11 and 12].

The employment of the hot wire in several types of experiments helped establish this result. First, both the Kovásznay [2] and the Morkovin [4] types of mode diagrams were made from data taken by the hot wire near the center line of the tunnel; these results are shown in Figs. 6 and 7. The mode diagram of Fig. 6 is similar to that presented in the first example. Again the mass flow and total temperature fluctuations are anti-correlated. After considering the many possible types of fluctuations that could be present in the flow field, consistent with the mode diagrams of Figs. 6 and 7, it is clear that the only possible *simple* fluctuation field is a pure sound field in which the isentropic relations between fluctuating quantities hold.

In a pure sound field the relation between the particle velocity normal to the wave front Δu_n and the pressure ΔP can easily be changed to a relation between the velocity variation in the direction of the mean flow Δu and ΔP. Of course, this relation is identical to the wavy wall solution found in the first example. In fact, the velocity for the sound field source may be determined from the relations derived in Example 1 by determining $\Delta u'$ and $\Delta P'$ as was done in Example 1.

Although the second type of mode diagram is not needed to completely determine the problem, this type of mode diagram will be presented to illustrate its application. The hot-wire equation for a pure sound field simplifies to [4]

$$\frac{\Delta e'}{\Delta e_\sigma} = \left(f + g \frac{\Delta e_\tau}{\Delta e_\sigma} \right) \pi'$$

where

$$f = -\frac{(\gamma - 1)(M^2 - 1)}{1 + (\gamma - 1) M^2}$$

$$g = \frac{\gamma(\gamma + n_x M) - (M^2 - 1)\dfrac{n_x}{M}}{1 + (\gamma - 1) M^2}$$

When

$$\frac{\Delta e_\tau}{\Delta e_\sigma} = 0, \qquad \pi' = \frac{\left(\dfrac{\Delta e'}{\Delta e_\sigma} \right)_0}{f}$$

which is the intercept on the ordinate axis. When $\Delta e'/\Delta e_\sigma = 0$,

$$g = \frac{-f}{\left(\dfrac{\Delta e_\tau}{\Delta e_\sigma} \right)_0}$$

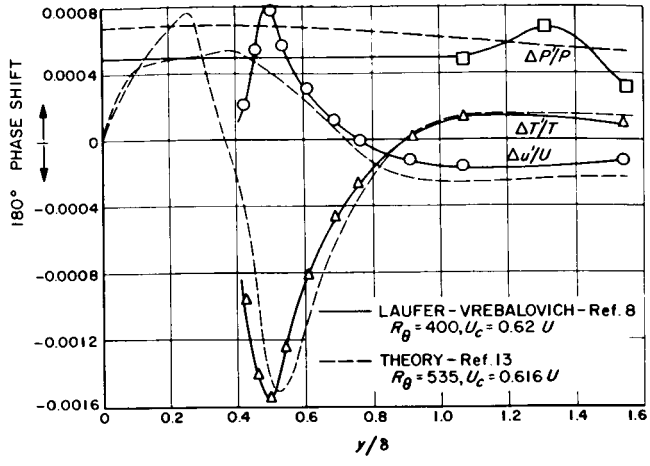

Figure 5. Velocity, temperature, and pressure fluctuations in a laminar boundary layer

which is the intercept on the abscissa axis.

Substituting in the definition of g given above and solving for n_x,

$$n_x = gM - \frac{\gamma M}{(\gamma - 1) M^2 - 1}$$

The direction that the wave front makes with the mean flow is

$$\theta = 180 \text{ deg} - \cos^{-1}(n_x)$$

The orientation of the waves and thereby the source velocity may now be determined:

$$\frac{U_r}{a} = \frac{U - U_c}{a} = -\frac{1}{\cos\theta}$$

where U_r is the relative velocity past a stationary source and U_c the source velocity in the boundary layer when the free-stream velocity is U. Then

$$\frac{U_c}{U} = 1 + \frac{1}{M \cos\theta}$$

and for $\theta = 180 \text{ deg} - \cos^{-1}(n_x)$,

$$\frac{U_c}{U} = 1 + \frac{1}{M n_x}$$

Therefore

$$\frac{U_c}{U} = 1 + \frac{1}{M n_x} = 1 - \frac{\dfrac{\Delta P'}{P}}{\gamma M^2 \dfrac{\Delta u'}{U}}$$

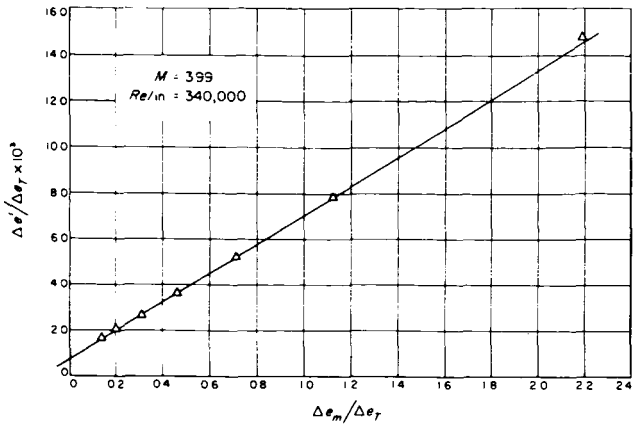

Figure 6. Fluctuation mode diagram, $\Delta e'/\Delta e_T$ vs $\Delta e_m/\Delta e_T$

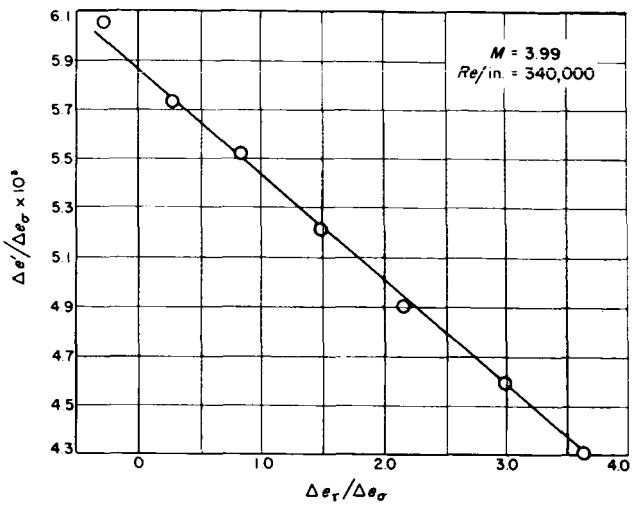

Figure 7. Fluctuation mode diagram, $\Delta e'/\Delta e_\sigma$ vs $\Delta e_T/\Delta e_\sigma$

The results of many of these measurements are plotted in Fig. 8.

A second method of determining the velocity of the disturbances in the boundary layer was simply to make a time correlation measurement between two hot wires in the flow field. This technique is comparable with the space correlation measurement in the first example, and the results are also presented in Fig. 8. The correlation measurements were made near the higher Reynolds number on Fig. 8 and the two methods of determining the source velocity gave comparable results.

It should be mentioned that the level of fluctuations in the tunnel increased with Mach number. At a given Mach number the amplitude of the fluctuations in the tunnel increased as the tunnel pressure and Reynolds number were decreased. The wall boundary layers increased in thickness with decreasing tunnel pressure until they became laminar. At this point the amplitude of the fluctuations sharply decreased. This provided further evidence that the wall boundary layers act as a source of moving disturbances which radiate sound into the free stream of the tunnel.

Conclusions

The measurement of the mean-square output of the fluctuating component of the voltage across a hot wire at different operating temperatures is the key to separating the components of an unsteady flow field in supersonic flow. This is a result of the fact that the sensitivity of the hot wire to the different fluctuating components is a function of the operating temperature of the wire. The separation of the fluctuating components into entropy, vorticity, and sound modes and the use of the fluctuation mode diagram to determine these modes aid in the determination of the unsteady parameters in supersonic flow fields.

The examples presented illustrate the use of mode diagrams. The problems described also were compared both with theory and with other measuring techniques and the results compare favorably.

The hot wire is shown to be a valuable tool in determining unsteady flow parameters in supersonic flow.

References

1. Kovásznay, L. S. G., "The Hot-Wire Anemometer in Supersonic Flow," *Journal of the Aeronautical Sciences*, 17(9): 565, September 1950.

2. Kovásznay, L. S. G., "Turbulence in Supersonic Flow," *Journal of the Aeronautical Sciences*, 20(10): 657, October 1953.

3. Kovásznay, L. S. G., *Development of Turbulence Measuring Equipment*, NACA TN 2839, January 1953.

4. Morkovin, M. V., *Fluctuations and Hot Wire Anemometry in Compressible Flows*, AGARDograph 24, November 1956.

5. Laufer, J. and McClellan, R., "Measurement of Heat Transfer from Fine Wires in Supersonic Flows," *Journal of Fluid Mechanics*, 1 (3): 276, September 1956.

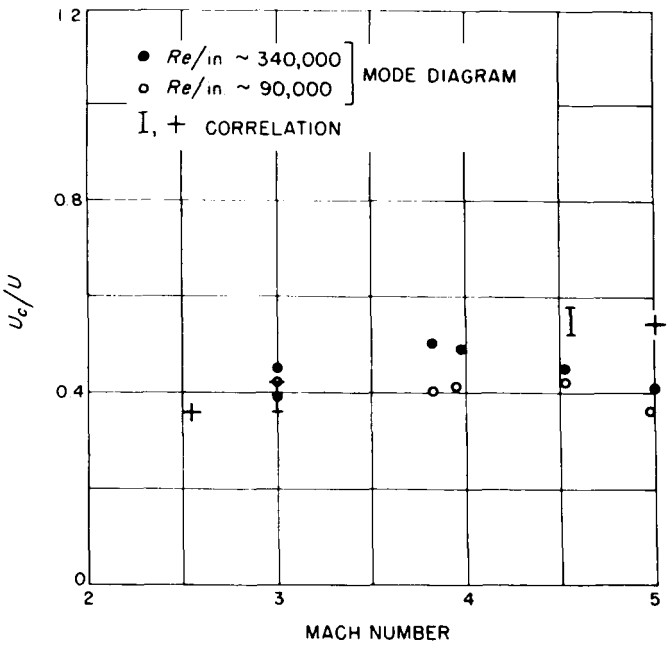

Figure 8. Variation of sound wave source velocity with tunnel Mach number

6. Spangenberg, W. G., *Heat Loss Characteristics of Hot-Wire Anemometers at Various Densities in Transonic and Supersonic Flow*, NACA TN 3381, May 1955.

7. Kistler, A. L., *Fluctuation Measurements in Supersonic Turbulent Boundary Layers*, Report No. 1052, Ballistic Research Laboratories, Aberdeen Proving Ground, Maryland, August 1958.

8. Laufer, J. and Vrebalovich, T., "Stability and Transition of a Supersonic Laminar Boundary Layer on an Insulated Flat Plate," *Journal of Fluid Mechanics*, 9(2): 257, 1960.

9. Laufer, J. and Vrebalovich, T., *Stability of a Supersonic Laminar Boundary Layer on a Flat Plate*, Report No. 20-116, Jet Propulsion Laboratory, Pasadena, California, December 1958.

10. Liepmann, H. W. and Roshko, A., *Elements of Gasdynamics*, John Wiley and Sons, New York, 1957.

11. Laufer, J., "Aerodynamic Noise in Supersonic Wind Tunnels," *Journal of the Aerospace Sciences*, 28(9): 685, September 1961.

12. Laufer, J., *Sound Radiation from a Turbulent Boundary Layer*, Technical Report No. 32-119, Jet Propulsion Laboratory, Pasadena, California, November 1961.

13. Lees, L., and Reshotko, E., *Stability of the Compressible Laminar Boundary Layer*, AGARD Report 268 presented at Boundary Layer Research Meeting of AGARD Fluid Dynamics Panel held in London, England, April 25-29, 1960.

14. Morkovin, M. V., and Phinney, R. E., *Extended Applications of Hot-Wire Anemometry to High-Speed Turbulent Boundary Layers*, AFOSR TN-58-469, Johns Hopkins University, Department of Aeronautics, June 1958.

APPENDIX

Computation of Hot-Wire Fluctuations

To begin the outline of the computational technique, the pertinent nomenclature and necessary data are given as follows:

M free-stream Mach number
T_T supply temperature, °K
P_T supply pressure, cm Hg
d diameter of wire, cm
l length of wire, cm
K_m heat conductivity of wire
K_T heat conductivity of air at T_T
R_L lead resistance
R_w heated resistance of wire
R_r recovery resistance of wire (unheated)
α_f first-order temperature coefficient of resistance at 0° C
γ_f second-order temperature coefficient of resistance at 0° C
i wire current

$$\left.\begin{aligned} n_T &= \frac{T_T}{K_T}\frac{dK_T}{dT_T} = 0.885 \\ m_T &= \frac{T_T}{\mu_T}\frac{d\mu_T}{dT_T} = 0.765 \end{aligned}\right\} \quad 270° \text{ K} < T_T < 350° \text{ K}$$

μ_T viscosity of air at T_T
M_T time constant of wire
$\Delta e'$ rms fluctuation of voltage across wire

$$\left.\begin{aligned} \gamma &= 1.4 \\ \alpha &= (1 + 0.2M^2) \\ \beta &= 0.4\,\alpha M^2 \end{aligned}\right\} \quad \text{for air}$$

1. Calculate Re_T: (Sutherland, viscosity)

$$Re_T = 0.636 \times 10^6 \frac{M}{(1 + 0.2M^2)^3} \frac{T_T + 110.2}{T_T^2} P_T d$$

2. From the Reynolds number determine *infinite length wire* Nusselt number Nu_∞ from the following empirical formulas:

For $M \geq 1.2$ and $Re_T < 16$,

$$Nu_\infty = 0.00268\, Re_T^2 - 0.0313\, Re_T^{3/2} + 0.154\, Re_T + 0.0423\, Re^{1/2} - 0.00528$$

For $M \geq 1.2$ and $Re \geq 16$,

$$Nu_\infty = -0.52 + 0.457\sqrt{Re_T}$$

3. Calculate the recovery temperature ratio term $\frac{Re_T}{\eta}\frac{\partial \eta}{\partial Re_T}$:

$$\eta = \frac{T_r}{T_T} = \eta(Re_T)$$

See Table A-1.

4. Calculate $\frac{M}{\eta}\frac{\partial \eta}{\partial M}$:

For $1.2 < M < 1.5$,

$$\eta = 0.95 + 0.043\,(1.5 - M)^{3/2}$$

For $M \geq 1.5$,

$$\frac{\partial \eta}{\partial M} = 0$$

5. For the end loss correction, calculate the following:

$$a_w' = \frac{R_w - R_r}{R_r}$$

$$R_f = \frac{R_r}{1 + \alpha_f (T_r - 273)}$$

$$\alpha_r = \alpha_f \frac{R_f}{R_r}, \qquad \gamma_r = \gamma_f \frac{R_r}{R_f}$$

Note that $R_w = R_f\{1 + \alpha_f(T_w - 273) + \gamma_f[\alpha_f(T_w - 273)^2]\}$ where T_w is the heated-wire temperature

$$K_T = (0.666 + 0.0187) \times 10^{-5}$$

End loss parameter:

$$\psi = \frac{d}{l}\sqrt{\frac{K_m}{K_T}}$$

Nu_m' = measured Nusselt number (see step 7)

Table A-1. Recovery temperature ratios for $M \geq 1.2$

Re_T	η	$-\frac{Re_T}{\eta}\frac{\partial \eta}{\partial Re_T}$
1	1.04	0.057
2	1.03	0.052
4	1.01	0.044
6	0.990	0.038
8	0.979	0.033
10	0.972	0.029
12	0.967	0.026
14	0.964	0.023
16	0.961	0.021
18	0.958	0.020
20	0.956	0.019
25	0.954	0.016
30	0.950	0.014
40	0.947	0.011
50	0.945	0.009
100	0.945	0

Nu'_m = Nusselt number determined by inverse end loss correction applied to infinite length wire

Nu_m should equal Nu'_m; this provides a check on the accuracy of the measurements.

$$Nu_m = Nu_\infty + \frac{0.6\,\psi^2}{1 + a'_w} + \frac{1.1\,\psi}{\sqrt{1 + a'_w}}\sqrt{Nu_\infty}$$

where Nu_∞ is found from step 2.

6. Calculate $\frac{Re_T}{Nu_m}\frac{\partial Nu_m}{\partial Re_T}$:

$$\frac{Re_T}{Nu_m}\frac{\partial Nu_m}{\partial Re_T} = \left[\frac{\sqrt{Nu_\infty(1 + a'_w)}}{\sqrt{Nu_\infty(1 + a'_w)} + 0.55\,\psi}\right]\frac{Re_T}{Nu_\infty}\frac{\partial Nu_\infty}{\partial Re_T}$$

where $\partial Nu_\infty / \partial Re_T$ is calculated from step 2.

7. Calculate e, τ_{wr}, Nu'_m, and K, where e = the dc voltage across the wire:

$$e = iR_w$$

$$\tau_{wr} = \frac{a'_w}{\alpha_r T_r}(1 - a'_w \gamma_r)$$

$$Nu'_m = \frac{0.239\,i^2 R_w}{\pi l K_T \tau_{wr} T_r} = \frac{0.239\,i^2 R_w \alpha_r R_r}{\pi l K_T (R_w - R_r)}$$

$$K = \frac{1}{1 + a'_w}\left[\alpha_r T_r + a'_w + a'_w \gamma_r (3\alpha_r T_r + 2a'_w)\right]$$

8. Calculate A'_w:

$$A'_w = \frac{1}{2}\frac{i}{R_w}\frac{\partial R_w}{\partial i}$$

Experimentally it is easier to determine A'_w from a plot of

$$\frac{i^2 R_w}{R_w - R_r} \text{ vs } a'_w = \frac{R_w - R_r}{R_r}$$

Within the scatter this plot is usually a straight line. From this plot determine c, where

$$c = -\frac{d\left(\frac{i^2 R_w}{R_w - R_r}\right)}{d\,a'_w}\frac{1}{\left(\frac{i^2 R_w}{R_w - R_r}\right)_{R_w = R_r}}$$

Then

$$A'_w = \frac{a'_w}{1 - (1 + a'_w)\frac{ca'_w}{1 - ca'_w}}$$

9. Calculate E':

$$\epsilon = \frac{R_w + R_L}{R_w + R_L + z}$$

$$E' = \frac{1 - \epsilon}{1 + 2A'_w \epsilon}$$

where R_L is the lead resistance and z is the ratio of the open circuit voltage to the short circuit current.

10. Calculate the time constant correction. The time constant equation is

$$M_T = \frac{c'}{0.239\ \alpha_r R_r}\ (1 - 2\gamma_r a'_w)\ \frac{A'_w}{i^2(1 + 2A'_w \epsilon)}$$

where c' is the thermal capacity of the wire. The time constant is determined by the square wave method for each overheat value; the above equation is used to check the experimental values rather than to determine absolute values.

Determine from the time constant equation

$$C_{T_m} = \frac{M_{T_m}\ \alpha_r R_r}{1 - 2\gamma_r a'_w}\ \frac{i^2(1 + 2A'_w \epsilon)}{A'_w}$$

where M_{T_m} is the measure time constant. If M_{T_m} is accurately determined, C_{T_m} will be the same for all overheat values at a given tunnel condition. Since this is not usually the case, an average C_T or a value that is averaged by eliminating the poorest measurements is determined. Then

$$M_{T_{(\text{corrected})}} = M_{T_m}\ \frac{C_{T_{(\text{average})}}}{C_{T_{(\text{measured})}}}$$

For the high frequencies encountered in supersonic flow fields, $\Delta e'$ may be corrected by the following [14]:

$$\Delta e' = \Delta e'_{(\text{measured})}\ \frac{M_{T_{(\text{corrected})}}}{M_{T_m}}$$

11. Calculate sensitivity coefficients:

$$\Delta e_\rho = eE'\left[A'_w\ \frac{Re_T\ \partial Nu_m}{Nu_m\ \partial Re_T} - \frac{A'_w}{\tau_{wr}}\ \frac{Re_T}{\eta}\ \frac{\partial \eta}{\partial Re_T}\right]$$

$$\Delta e_u = \Delta e_\rho + eE'\left[\frac{A'_w}{\alpha}\left(\frac{M\ \partial Nu_m}{Nu_m\ \partial M} - \frac{1}{\tau_{wr}}\ \frac{M}{\eta}\ \frac{\partial \eta}{\partial M}\right)\right]$$

$$\Delta e_T = eE'\left[K + A'_w\left(K - 1.885 + 0.765\ \frac{Re_T}{Nu_m}\ \frac{\partial Nu_m}{\partial Re_T} + \frac{1}{2\alpha}\ \frac{M}{Nu_m}\ \frac{\partial Nu_m}{\partial M}\right) - \frac{A'_w}{\tau_{wr}}\left(0.765\ \frac{Re}{\eta}\ \frac{\partial \eta}{\partial Re} + \frac{1}{2\alpha}\ \frac{M}{\eta}\ \frac{\partial \eta}{\partial M}\right)\right]$$

$$\Delta e_\sigma = \Delta e_\rho + \alpha \Delta e_T$$

$$\Delta e_\tau = \beta \Delta e_T - \Delta e_u$$

12. Calculate and plot the following:

$$\frac{\Delta e'}{\Delta e_T} \text{ vs } \frac{\Delta e_\rho}{\Delta e_T}$$

$$\frac{\Delta e'}{\Delta e_\sigma} \text{ vs } \frac{\Delta e_\tau}{\Delta e_\sigma}$$